Supplement of

Modulation of Saharan dust export by the North African dipole

S. Rodríguez et al.

Correspondence to: S. Rodríguez (srodriguezg@aemet.es)

S1. Dust measurements

Measurements of in-situ aerosol dust concentrations have been performed at the Izaña Global Atmospheric Watch (GAW) observatory since 1987 (*http://www.wmo.int/pages/prog/arep/gaw/gaw_home_en.html*). These measurements are part of the in-situ aerosols GAW program in operation at Izaña, which also include long-term measurements of other aerosol properties (chemical composition, size distribution and optical properties) (*http://www.wmo.int/pages/prog/arep/gaw/aerosol.html*).

The Izaña observatory is located on Tenerife island (28° 18'N, 16° 29'W; the Canary Islands) at 2367 meters above the sea level. The site is normally above the marine stratocumulus associated with the trade winds inversion layer, typical of the subtropics. At night, when upslope winds cease, Izaña is exposed to the free troposphere airflows.

Samples of atmospheric aerosols are collected by drawing the ambient air through a filter mounted in a sampler whose pump operates at a controlled (constant) airflow. Subsequently, these samples are subject to chemical analysis for determining the concentrations of dust and other aerosol species (Table S1). These analyses have been performed in several size fractions of ambient aerosols:

(a) Total Particulate Matter (PM_T). A sampler with a whole air inlet operating at 30 to 50 m^3/h airflow, depending on the period, was used.

(b) Particulate Matter with an aerodynamic diameter smaller than 10 microns (PM_{10}). The sampling was performed at 30 m^3/h flow-rate placing an impactor, equivalent to the EN–12341 standard, in the inlet of the sampler.

(c) Particulate Matter with an aerodynamic diameter smaller than 2.5 microns ($PM_{2.5}$). The sampling was performed at 30 m^3/h flow-rate placing an impactor, designed according to EN–14907 standard, in the inlet of the sampler.

Dust concentrations are extracted from the chemical composition dataset (Table S1) in three size fractions:

1. Concentrations of total dust ($dust_T$), obtained by chemical analysis of the PM_T samples.

2. Concentrations of dust particles with an aerodynamic diameter smaller than 10 microns ($dust_{10}$), obtained by chemical analysis of PM_{10} samples.

3. Concentrations of dust particles with an aerodynamic diameter smaller than 2.5 microns ($dust_{2.5}$), obtained by chemical analysis of $PM_{2.5}$ samples.

The long-term observations of size segregated dust concentrations at Izaña have been based on the following measurements:

- 1987–1999: based on $dust_T$.

- 2000–2001: no measurements available.

- 2002–2004: based on $dust_T$ and $dust_{2.5}$.

- 2005–2014: based on $dust_{10}$, $dust_{2.5}$ and $dust_T$ (the latter only in August, the month in which dust events occur with the highest frequency).

In order to avoid a large volume of data in the plots, in the Article we only presented data of $dust_T$ and $dust_{2.5}$.

During the 1987–1999 period, sampling was performed almost every day. In the 2002–2014 period, sampling was performed at the rate of 1 sample collection every 3 to 4 days in two size fractions, except in August, when the sampling was performed every day in the three size fractions.

Complementary size distributions measurements were performed with an optical particle counter (GRIMM™, 1108) since 2002 and an aerodynamic particle sizer (TSI™, model 3321) since 2006 in the size range 0.5 to 20 microns. We used these data for estimating the bulk aerosol mass concentrations in several size factions with an hourly resolution. Volume aerosol concentrations (determined from the number size distributions) were converted to mass aerosol concentrations using standard methods (Rodríguez et al., 2012). We used a volume to mass conversion factor (effective density equivalent) obtained by correlating and fitting by regression of the aerosol dust concentrations obtained by chemical methods versus aerosol volume concentrations. This method was applied in the three size fractions: total particles and particles smaller than 10 μm and 2.5 μm.

Figure S1: Saharan dust samples. Examples of batch of filters with aerosol samples collected at Izaña for illustrating their typical ochre color due to dust.

Table S1: Description of the sampling and chemical analysis of the aerosol samples.

<u>1987 to 1999.</u>
Samples of Total Particulate Matter (PM_T) were collected on 20 cm by 25 cm Whatman 41 paper filters at a nominal flow rate of about 35 m^3/h. In 1994 the airflow was modified to 50 m^3/h. Samples were stored and sent periodically to the University of Miami. Blank field filters were also chemically analyzed. Dust concentrations records with the following method are available for 4460 days.

- Concentrations of soluble species were determined by extraction with de-ionized water subsequent analysis by flame atomic absorption (Na^+), ion chromatography (Cl^-, NO_3^- and $SO_4^=$) and colorimetry (NH_4^+).

- Concentrations of aluminium were analyzed by Instrumental Neutron Activation Analysis.

- Dust concentrations. The extracted filters were placed in a muffle furnace for 14-h (overnight) at 500 °C.

After blank removal, the ash residue weight divided by the sampled volume is the mineral dust concentration. Because the scatter plot of Al versus dust typically shows a slope of 10.4 %, which is somewhat higher than the mean content of Al in soils (8 %), a normalization factor of 1.3 was used (Arimoto et al., 1995). Standard error is considered $\pm 0.1 \mu g/m^3$ for concentrations $<1 \mu g/m^3$, and about 10 % for higher concentrations.

<u>2002 to 2014.</u>
Aerosol samples in several size fractions were collected at the flow rate of 30 m^3/h in micro quartz fibre filter Schleicher & Schuell™ QF20 (2002–2006) and Munktell™ MK360 (2007–2014). Filters were weighed before and after sampling following the EN–14907 procedure (except for relative humidity, which was set to 30-35 % in the weighing room). Samples were stored and sent periodically to the Research Council of Spain (CSIC) in Barcelona for chemical analysis. Chemical composition data obtained with the following method is available during 652 days. Blank field filters were also chemically analyzed.

- Concentrations of soluble species were determined by extraction in de-ionized water subsequent analysis by ion chromatography (Cl^-, NO_3^- and $SO_4^=$) and FIA colorimetry (NH_4^+).

- Concentrations of major elements (Al, Ca, K, Na, Mg and Fe) and trace elements were determined by acid digestion ($HF:HClO_4:HNO_3$) and subsequent Inductively Coupled Plasma Atomic Emission Spectrometry, (ICP-AES, IRIS Advantage TJA Solutions, THERMO), and Inductively Coupled Plasma Mass Spectrometry, (ICP-MS, X Series II, THERMO), respectively. Detection limit and accuracy were estimated as 0.4 ng/m^3 and 2 % for ICP-AES and 0.02 ng/m^3 and 3 % for ICP-MS.

- <u>Dust concentrations</u> were determined as the sum of $Al_2O_3 + SiO_2 + Fe + CaCO_3 + K + Na + P + Ti + Sr$. The following indirect determinations were used: (a) CO_2^{3-}, calculated from the amount of Ca not present as Ca-sulphate and Ca-nitrate, and then assuming this fraction of Ca is present as calcite ($CaCO_3$; $CO_3^= = 1.5Ca$; Rodríguez et al., 2011); (b) SiO_2, determined from the Al content on the basis of prior experimental equations ($SiO_2 = 3*Al_2O_3$, see Querol et al., 2001). Data were normalized in order that the mean Al content in the aerosol dust be 8 %, as also performed in the 1987–1999 dataset.

- Carbonaceous aerosols were characterized in terms of total carbon (TC) and organic carbon (OC) and elemental carbon (EC). Concentrations of TC were determined with a Total Carbon Analyser (LECO) from 2002 to 2007. Concentrations of OC and EC were analyzed since 2007 by a thermal-optical transmission technique (Birch et al., 1996) using a Sunset Laboratory OC-EC analyzer.

The differences in the daily average dust concentrations data obtained with these two methods (based on chemical analysis and on size distributions) is within the range 3–8 %. The good agreement between these two methods (high linearity and low mean bias) is due to the very low aerosol volume concentrations in the free troposphere during no dust events (typically < 1 to 2 μm^3/cm^3; Rodríguez et al., 2009) and to the fact that the aerosol volume concentrations during dust events are by far dominated by dust, as evidenced by the chemical analysis (Rodríguez et al., 2011) and the ochre color of the sampled filters (Fig. S1). As part of the quality control in data analysis, we used monthly mean concentrations data obtained with the two methods for assessing the consistency of the monthly mean variations of dust concentrations.

During the whole measurement period (25 July 1987–31 December 2014, excluding the none-measurement period 11 October 1999–13 February 2002), dust concentrations records are available during 8001 days, which lead to a data availability of 87.3 %. Data collected at Izaña in different periods have been analyzed in individual studies, e.g. 1987–1999 (Chiapello et al., 1999), 2002 (Alastuey et al., 2005) and 2005 to 2008 (Rodríguez et al., 2011). All data were joined for the first time for this study.

The Quality Assurance/Quality Control activities of the Izaña aerosol program include periodic checks of airflows and zeros in all devices, collection of blank field filters and instrument inter-comparisons. The latter are typically performed during the summer dust season, when each sampling of PM$_T$, PM$_{10}$ and PM$_{2.5}$ is simultaneously performed with two samplers. PM$_x$ concentrations obtained with the two samplers typically differs 2–9 % for PM$_T$, and 3 % for PM$_{10}$ and PM$_{2.5}$.
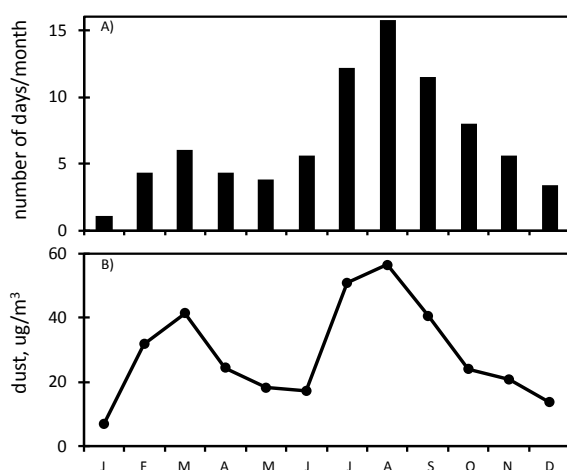
S2. Summer dust time series

At Izaña, the summer dust season (impacts of the Saharan Air Layer) typically starts in the second half of July and ends at the beginning of September (Fig. S2). The maximum frequency of dust events occurs in August (Fig. S2a). We used dust averaged in August (excluding July and September) for studying the long-term summer dust variability for the following reasons:

1. this is the only month when dust$_T$ concentrations were measured after 2004,

2. this is the only month when simultaneous dust$_T$, dust$_{10}$ and dust$_{2.5}$ measurements are available,

In August, the Inter-Tropical Convergence Zone (ITCZ) is shifted to the North and (i) the Saharan Air Layer is exported at the northern most latitude, as evidenced by the highest frequency of dust impacts at Izaña (Fig. S2a), and (ii) maximum rainfall occurs in tropical North Africa (Nicholson et al., 2009).

The high correlation of August mean dust concentrations with the July to September dust mean concentrations evidences that summer mean dust concentrations are mainly weighted by August (Fig. S3a). This is also true for dust annual mean (Fig. S3b). In August 1987–2014, daily dust data were available during 761 days, i.e. a data availability of 94 % (excluding the no-measurements period 11 October 1999–13 February 2002).
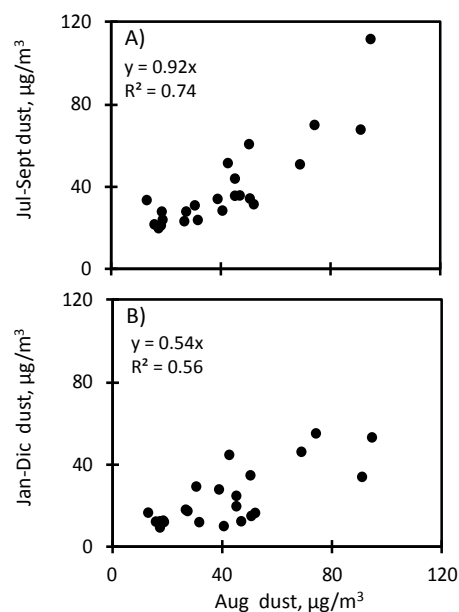

Figure S2: Statistics of dust events at Izaña from 1987 to 2014. A) Frequency of dust (> 10 μg/m^3) events; B) Average dust concentrations per month.

Figure S3: Scatter plots of summer and annual versus August dust means. A) Jul–Sept and (B) Jan–Dec versus Aug average dust concentrations at Izaña. Data corresponds to the period 1987–2014, based on dust$_T$ from 1987 to 2004, and on dust$_{10}$ from 2005 to 2014.
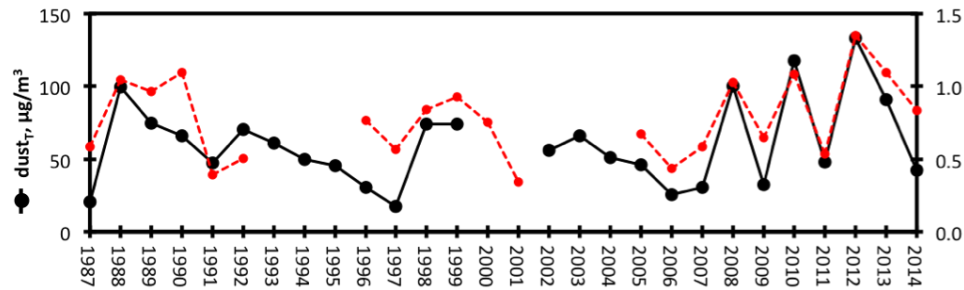
Figure S4: In-situ and satellite-AI dust signal over Izaña. Times series of summer mean $dust_T$ at Izaña and AI at the lat-lon of Izaña. The Pearson correlation coefficient (r) is shown in the plot.

S3. Supplementary data analysis

Table S2 shows the summer mean dust concentrations at Izaña from 1987 to 2014. For analyzing the large-scale processes influencing the inter-annual dust variability we used the following complementary data sets:

1. UV Aerosol Index (AI) data from the Total Ozone Mapping Spectrometer – TOMS – (1979–2001) and from the Ozone Monitor Instrument – OMI – (2005–2014) spectrometers onboard the satellites Nimbus 7 (TOMS 1979–1993), Earth Probe (TOMS 1996–2001) and Aura (OMI 2005–2014).

2. Back-trajectories calculated with the HYbrid Single-Particle Lagrangian Integrated Trajectory (HYSPLIT) model (Draxler and Rolph, 2013) developed by the NOAA Air Resources Laboratory (*http://www.arl.noaa.gov/*). Ten-day back-trajectories were calculated using National Center for Atmospheric Research (NCEP) data.

3. Gridded meteorological National Center for Environmental Prediction / National Center for Atmospheric Research (NCEP/NCAR) re-analysis data (Kalnay et al., 1996) were used for determining the North AFrican Dipole Index (NAFDI), equation 1 of the article.

4. Teleconnection index data downloaded from the NOAA-ERSL web (*http://www.esrl.noaa.gov/psd/data/climateindices/*).

These four data sets were subject to the following analysis.
We <u>first</u> analyzed the consistency between dust detection by the satellite AI signal and the in-situ dust measurements at Izaña. Previous studies found a high consistency between the variability in daily in-situ dust concentrations at Izaña and the daily AI signal at the lat-lon of Izaña (Chiapello et al., 1999). We found that there is also a high correlation between the long-term (1987–2014) in-situ $dust_T$ concentrations at Izaña and AI signal which supports the consistency between the two complementary dust observations techniques (Pearson correlation coefficient r=0.82; Fig. S4). We also assessed how the change of the

Table S2: Summer mean dust concentrations from 1987 to 2014 in three size fractions at Izaña observatory, and NAFDI index. Dust concentrations are normalized to 1013 hPa.

	$dust_T$ $\mu g/m^3$ average	$dust_{2.5}$ $\mu g/m^3$ average	$dust_T$ $\mu g/m^3$ Std Dev.	$dust_{2.5}$ $\mu g/m^3$ Std Dev.	NAFDI
1987	20.63		24.49		-2.79
1988	99.28		101.81		0.68
1989	74.52		60.34		-0.51
1990	66.23		51.81		0.30
1991	47.27		71.02		0.43
1992	70.05		90.43		0.48
1993	60.75		162.41		-1.34
1994	49.99		85.69		0.89
1995	45.15		43.17		-1.30
1996	30.54		43.33		-2.05
1997	17.36		21.24		-3.20
1998	74.14		88.89		0.00
1999	73.76		82.31		-1.14
2000					0.84
2001					-0.24
2002	56.01	19.32	47.28	8.28	-2.11
2003	66.15	15.71	24.03	5.18	-0.20
2004	51.10	15.87	44.91	8.64	-0.71
2005	43.41	14.17	48.32	13.02	-0.24
2006	24.48	9.96	23.67	8.63	-1.55
2007	29.34	9.61	31.52	9.71	-1.12
2008	99.84	23.43	64.55	16.49	1.02
2009	32.18	11.55	35.48	9.74	-0.36
2010	117.56	27.11	98.22	21.25	0.52
2011	47.83	15.74	57.37	13.53	0.30
2012	133.00	25.05	93.22	15.31	2.29
2013	90.91	27.63	59.92	28.64	0.33
2014	42.41	14.67	45.20	19.00	0.34

TOMS to the OMI sensor may have influenced the assessment of the spatial variability of dust that was performed in Fig. 4b of the Article. For this reason we performed the same analysis but only using data from the TOMS period (1979–2001).
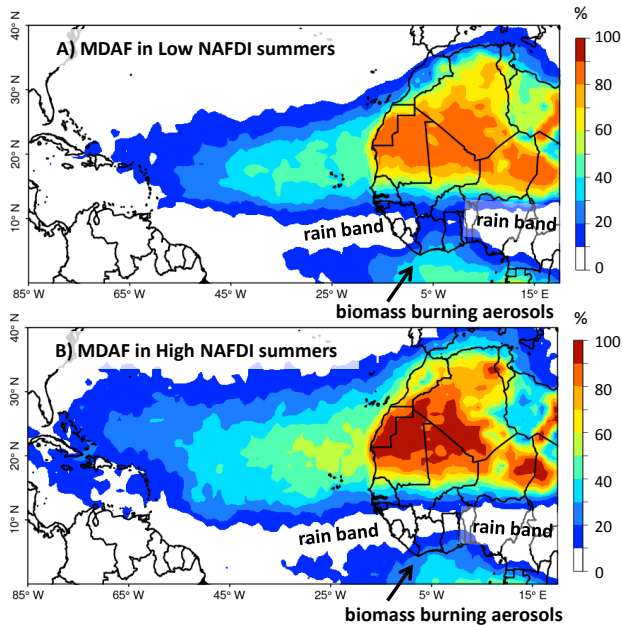
Figure S5: Spatial distribution of dust. MDAF studied using only TOMS data in summers of **(A)** low NAFDI (1981 = -1.7, 1983 = -2.6 and 1997 = -2.8) and **(B)** high NAFDI (1980 = +0.9, 1988 = +1.0 and 2000 = +0.8).

The main features of dust distribution during low and high NAFDI years observed with TOMS and OMI data (Fig. 3b of the Article) are also observed when only using TOMS data (Fig. S5). This is in agreement with the previously described consistency of the TOMS and OMI AI data already demonstrated by Li and co-workers (Li et al., 2009).

As a second step, we used the back-trajectories for identifying the North African regions that are potential dust sources and/or within the transport pathways of the dust recorded at Izaña. Fig. S6a shows the back-trajectories associated with the dust events $> 10 \, \mu g/m^3$ at Izaña from 1987 to 2014. The frequency of the back-trajectory passes (only considering points below 3000 m a.s.l.) in shown in Fig. S6b (see Rodríguez et al., 2011 for methodology). This trajectory analysis shows that dust at Izaña, and consequently the northern Saharan Air Layer, is sensitive to dust mobilization in a region that extends from Central Algeria through Northern Mauritian and Western Sahara, where important dust sources are located (Prospero et al., 2002).

Thirdly, we used the NCEP/NCAR re-analysis data and the NAFDI for studying the variability in the large-scale processes that influence long-term dust variability. The NAFDI typically exhibits values between -3 and +3 (Table S2). The implications of the variation of this index on the North African meteorological scenarios were described in the Article. Some plots (e.g. Fig. 2 of the Article) were created in

the NOAA– ESRL – Monthly/Seasonal Climate Composites web (*http://www.esrl.noaa.gov/psd/cgi-bin/data/composites/printpage.pl*). The intensification of the anticyclone in northern Sahara and the lower height of geopotential fields in all standard pressure levels in tropical North Africa result in the airflows characteristic of the high NAFDI summers described in the Article.
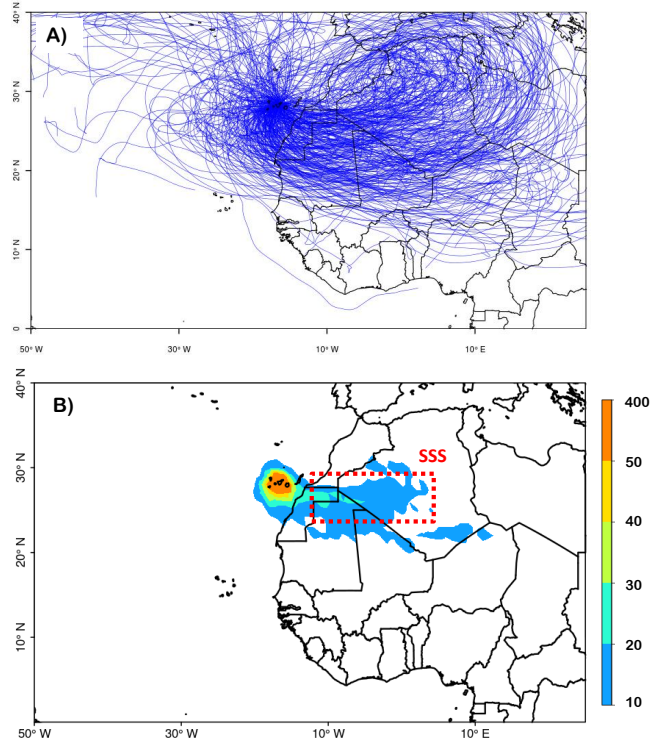

Figure S6: Transport pathways of dust. **A)** back-trajectories at Izaña during the dust events $> 10 \, \mu g/m^3$ registered in August from 1987 to 2014. **B)** frequency by which the points of the back-trajectories passes (in total counts).

We correlated the NAFDI with several meteorological fields (zonal and meridional component of wind in standard levels, precipitation rates, temperature and sea surface temperature – SST –, among others) during the 1987 to 2014 period. This was done in the NOAA-ESRL-Linear Correlations in Atmospheric Seasonal/Monthly Averages web (*http://www.esrl.noaa.gov/psd/data/correlation/*). Only relevant results for understanding dust inter-annual variability are shown. The NAFDI shows a high correlation (r > 0.8) with the zonal component of wind at the north of the ITCZ, in the subtropical Saharan Stripe (SSS) region, which extends from Central Algeria through Northern Mauritania to Western Saharan between 24 and 30 °N (Fig. 6a of the Article).

Long-term summer mean dust$_T$ at Izaña also showed a high correlation with the zonal component of wind at 925 hPa (r=0.65; Fig. 2b of the Article) and at 700 hPa in the SSS (r=0.79; Fig. 2c of the Article ; mean winds 1987–2014 in the SSS were calculated in the NOAA-ESRL web ; *http//www.esrl.noaa.gov/psd/data/timeseries/*). These results are consistent with the back-trajectories analysis described above, which also indicate that dust mobilization in the SSS exerts an important influence on dust records at Izaña (Fig. S6b).

The correlation analysis was also performed to assess the influence of NAFDI on rainfall in tropical North Africa. The NAFDI shows a positive correlation with gridded precipitation rates over the tropical North African and part of the Sahel (Fig. 6c of the Article). Although the correlation coefficient values are not very high (0.2 to 0.5, Fig. 6c of the Article), it is remarkable that this correlation is observed over an extension of thousands of square kilometers. Because of this, we then quantified the area of the Sahel was wet during the monsoon season. We defined "Wet Sahel Portion" as the area of the Sahel (14–18°N to 17°W–22.5°E) which received a mean precipitation rate $\geq$ 3 mm/day. Data of mean precipitation rates were downloaded from the NOAA-ESRL web. The Wet Sahel Portion showed a significant variability, from less than 5 % in dry periods up to 15 % in wet periods (Fig. 2d of the Article).

In a <u>fourth</u> step, we correlated the NAFDI and dust$_T$ at Izaña with other teleconnection indexes (Table S3). The NAFDI only shows a significant correlation with the Multivariate ENSO Index (MEI), which, in turn, is negatively correlated with dust at Izaña and with Sahel rainfall.

Table S3: Correlation coefficient between dust$_T$ at Izaña and NAFDI with a set of selected climate indexes. Data: mean values of August from 1987 to 2014. Bold: absolute values $\geq$ 0.5. Data source: Sahel Rainfall downloaded from the website of the Joint Institute for the Study of the Atmosphere and Ocean of the University of Washington (*http://jisao.washington.edu/data/sahel/#values*) NAO, TNA, MEI, SOI, El Niño 4, El Niño 3.4, El Niño 3 and El Niño 1+2 downloaded from the NOAA-ERSL web (*http://www.esrl.noaa.gov/psd/data/climateindices/*).

Physical meaning:

NAFDI	Differences of 700 hPa geopotential anomalies between central Morocco and Bamako region.
Wet Sahel Portion	Proportion (%) of Sahel that received a precipitation rate $\geq$ 3 mm/d.
Sahel Rainfall	Precipitation anomaly with respect to 1950–79.
NAO	Normalized pressure differences between Azores and Iceland.
TNA	Anomaly of the average of the monthly SST from 5.5N to 23.5N and 15W to 57.5W.
MEI	Based on six variables over the tropical Pacific: sea-level pressure, zonal and meridional components of the surface wind, sea surface temperature, surface air temperature and total cloudiness fraction of the sky.
SOI	(Stand Tahiti - Stand Darwin) Sea Level Pressure.
El Niño 4	Central Tropical Pacific SST *(5N–5S) (160E–150W).
El Niño 3.4	East Central Tropical Pacific SST* (5N–5S)(170–120W).
El Niño 3	Eastern Tropical Pacific SST (5N–5S,150W–90W).
El Niño 1+2	Extreme Eastern Tropical Pacific SST *(0–10S, 90W–80W).

In a <u>fifth</u> and final step, we used AI data for assessing how the NAFDI influenced the spatial distribution of dust in the North Atlantic. We found that increases in the values of the NAFDI enhance dust export at subtropical latitudes. This is clearly observed in the plots of the 'correlation coefficient between NAFDI and MDAF and dust$_T$ at Izaña' (Fig. 7 of the Article).

S4. Supporting References

Alastuey, A., Querol, X., Castillo, S., Escudero, M., Avila, A., Cuevas, E., Torres, C., Romero, P., Exposito, F., and Garcia, O.: Characterisation of TSP and PM$_{2.5}$) at Izaña and Sta. Cruz de Tenerife (Canary Islands, Spain) during a Saharan dust episode (July 2002), Atmos. Environ., 39(26), 4715–4728, doi:10.1016/j.atmosenv.2005.04.018, 2005.

Arimoto, R., Duce, R. A., Ray, B. J., Ellis, W. G., Cullen, J. D. and Merrill, J. T.: Trace elements in the atmosphere over the North Atlantic, J. Geophys. Res., 100, 1199–1213, doi:10.1029/94JD02618, 1995.

Birch, M. E. and Cary, R. A.: Elemental carbon-based method for monitoring occupational exposures to particulate diesel exhaust, Aerosol Sci. Tech., 25, 221–241, doi:10.1080/02786829608965393, 1996.

Chiapello, I., Prospero, J. M., Herman, J. R. and Hsu, N. C.: Detection of mineral dust over the North Atlantic Ocean and Africa with the Nimbus 7 TOMS, J. Geophys. Res., 104, 9277–9291, doi:10.1029/1998JD200083, 1999.

http://jisao.washington.edu/data/sahel/#values, last access: 20 February 2015

http://www.arl.noaa.gov/, last access: 20 February 2015

http://www.esrl.noaa.gov/psd/cgi-bin/data/composites/printpage.pl, last access: 20 February 2015

http://www.esrl.noaa.gov/psd/data/climateindices/, last access: 20 February 2015

http://www.esrl.noaa.gov/psd/data/correlation/, last access: 20 February 2015

http://www.esrl.noaa.gov/psd/data/timeseries/, last access: 20 February 2015

http://www.wmo.int/pages/prog/arep/gaw/aerosol.html, last access: 20 February 2015

http://www.wmo.int/pages/prog/arep/gaw/gaw_home_en.html, last access: 20 February 2015

Querol, X., Alastuey, A., Rodríguez, S., Plana, F., Mantilla, E. and Ruiz, C. R.: Monitoring of PM$_{10}$ and PM$_{2.5}$) around primary particulate anthropogenic emission sources, Atmos. Environ., 35, 845–858, doi:10.1016/S1352-2310(00)00387-3, 2001.

phenomenon	index name	dust$_T$ Izaña 1987–2014	NAFDI 1987–2014	NAFDI 1950–2014
North African dipole	NAFDI	**0.72**		
Sahel rainfall	Wet Sahel Portion	**0.74**	**0.54**	
Sahel rainfall	Sahel Rainfall	**0.58**	**0.55**	0.43
North Atlantic Oscillation	NAO	-0.24	-0.14	-0.19
Tropical North Atlantic	TNA	-0.37	-0.30	-0.24
Multivariate ENSO Index	MEI	**-0.59**	**-0.50**	-0.44
ENSO	SOI	**0.59**	0.45	0.38
ENSO	El Niño 4	**-0.60**	-0.35	-0.31
ENSO	El Niño 3.4	**-0.56**	-0.44	-0.33
ENSO	El Niño 3	-0.44	-0.46	-0.42
ENSO	El Niño 1+2	-0.35	-0.43	-0.45